East European Journal of Physics. 2. 394-397 (2024)
DOI:10.26565/2312-4334-2024-2-50 ISSN 2312-4334

SPECIFIC FEATURES OF CARBON NANOPARTICLE FORMATION UNDER THE INFLUENCE OF A LASER OPERATING IN A DOUBLE-PULSE GENERATION MODE

Maria I. Markevich[a], Amangeldi B. Kamalov[b], Dauran J. Asanov[b]*, Daryabay M. Esbergenov[c], Manzura A. Kazakbaeva[b]

[a]*Physico-Technical Institute of the National Academy of Sciences of Belarus, Minsk*
[b]*Nukus State Pedagogical Institute Named After Ajiniyaz, Nukus, Republic of Karakalpakstan*
[c]*Nukus Branch of Tashkent University of Information Technologies Named After al-Khwarizmi, Republic of Karakalpakstan*
**Corresponding Author e-mail: dauranbek83@list.ru*
Received April 1, 2024; revised April 21, 2024; accepted May 6, 2024

This study investigates the morphology of carbon nanoparticles generated through the ablation of an MPG-6 carbon target in an aqueous environment. The ablation process utilized an LS-2134D aluminum yttrium garnet laser (wavelength: 1064 nm) operating in a double-pulse mode (pulse separation: 3 µs, pulse duration: 10 ns, pulse repetition rate: 10 Hz, single pulse energy: ~0.05 J). The results demonstrate the formation of a diverse range of carbon nanoparticles with varying sizes and shapes during laser ablation. Additionally, the study showcases the ability to control the ablation process and subsequent synthesis of carbon nanoparticles, achieving efficient generation of nanoparticles suitable for various applications.
Keywords: *Nanoparticles; Laser irradiation; Nanosecond pulse duration; Double-pulse regime; Carbon*
PACS: 42.55.Ye, 61.82.Rx, 78.67.Bf

INTRODUCTION

Currently, numerous scientists both abroad and within our country are increasingly employing various forms of carbon for the high-temperature synthesis of SHS materials. It has been established that obtaining graphite particles of different sizes can be utilized to control the SHS reaction [3].

Furthermore, carbon particles are extensively used as pigment fillers and additives to enhance the strength and electrical conductivity of materials. The production of various cable and wire products typically involves the use of carbon particles. The diversity of colors in polymer materials is achieved by varying the size and concentration of carbon particles [1-4].

Among the various methods for modifying the surface of graphite, laser treatment, particularly in a two-pulse mode, remains significantly understudied [5-6].

In our work, we will explore the production of carbon particles of different sizes using laser ablation. Laser ablation offers vast potential for obtaining nanoparticles in solutions, as the particles produced by this method are characterized by high purity. This is based on the unique properties of laser radiation: coherence, monochromaticity, short duration of exposure, high energy densities in the pulse, absence of direct contact between the material and the energy source, sterility of the process, and the rapid nature of the method. Laser ablation of various substances in liquids has been investigated in studies [9-10].

MATERIAL AND METHOD

Sample analysis was conducted using a Hitachi S-4800 scanning electron microscope (SEM). For material processing, an yttrium aluminum garnet (YAG) laser (LS-2134D) with a wavelength of 1064 nm was employed. The laser operated in a two-pulse mode with the following parameters: Pulse separation: 3 µs, pulse duration: 10 ns, pulse repetition rate: 10 Hz single pulse energy: ~0.05 J, exposure time: 60 minutes, power density range: $1.3\text{-}2\times10^7$ W/cm² [7-8]. The object of investigation was an MPG-6 carbon target submerged in distilled water. The liquid was not forcibly stirred. The sample dimensions were: Length: 20 mm, width: 10 mm, thickness: 3 mm

DESCRIPTION AND ANALYSIS OF RESULTS

Table 1 presents the key characteristics of MPG-6 Graphite Composite, outlining its physical and electrical properties. The data reveals that MPG-6 exhibits a combination of desirable features, including:

Good electrical conductivity: With a specific electrical resistivity of 11-16 µΩ·m, MPG-6 demonstrates its ability to conduct electricity efficiently, making it suitable for applications where electrical conductivity is crucial.

Lightweight nature: Its bulk density of 1.76-1.88 g/cm³ signifies that MPG-6 is relatively lightweight compared to many metals, offering potential advantages in weight-sensitive applications.

High purity: The low ash content of 0.25-0.1% indicates a high degree of purity in the composite, which can be important for specific applications.

Cite as: M.I. Markevich, A.B. Kamalov, D.J. Asanov, D.M. Esbergenov, M.A. Kazakbaeva, East Eur. J. Phys. 2, 394 (2024), https://doi.org/10.26565/2312-4334-2024-2-50

Stiffness and strength: While not as stiff as some metals, the Young's modulus of 10-12 GPa demonstrates that MPG-6 maintains respectable stiffness and strength.

Porous structure: The 9% porosity indicates the presence of some void space within the material. This characteristic may influence its behavior in certain applications, and further investigation into its implications could be beneficial. By presenting these properties, Table 1 provides valuable insights into the nature of MPG-6 Graphite Composite, aiding in the understanding of its potential applications and limitations.

Table 1. Characteristics of MPG-6 Graphite Composite

	Units of Measurement	MPG -6
Specific electrical resistivity	μΩ·m	11-16
Bulk density	g/cm³	1,76-1,88
Porosity	%	9
Ash content	%	0,25-0,1
Grain size	μm	30-150
Young's modulus	GPa	10-12

Data on the phase composition of the irradiated graphite surface were obtained from the analysis of Raman scattering (RS) spectra at a wavelength of 532 nm. The RS spectra were measured using a spectral-analytical complex based on a Nanofinder High End scanning confocal microscope from LOTIS-TII (Belarus-Japan). The RS spectra were excited by a line of a solid-state Nd laser with a wavelength of 532 nm and recorded at room temperature. A cooled CCD camera served as the detector. The probing spot had a diameter of 1 μm [9-20].

When a series of nanosecond laser pulses is applied to the surface of a carbon sample located in water, a region consisting of water vapor, products of an erosive laser torch, is formed near the surface. The ablation plasma formed as a result of the evaporation of a substance under the influence of the first pulse creates an area in the near-surface layer with an increased temperature and a reduced density of particles, which leads to a more complete use of the energy of the second pulse for laser ablation [12-15].

Figure 1 shows micrographs of carbon nanoparticles obtained using SEM at various magnifications. Formed as a result of laser exposure. Power density 1.67×10^{7} W/cm², exposure time 60 min.

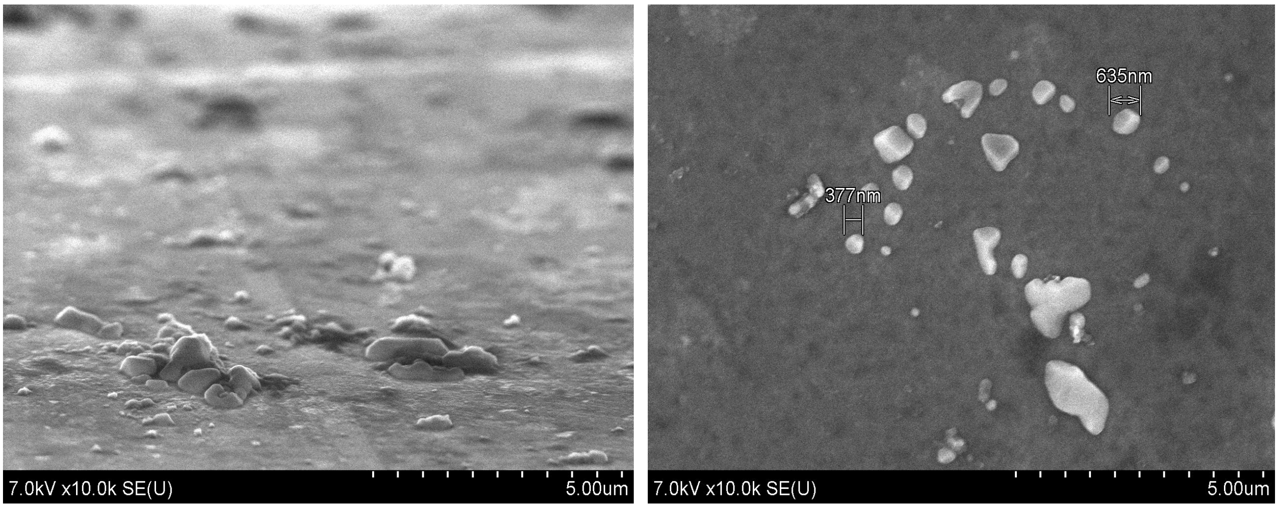

a *b*

Figure 1. Surface morphology of carbon nanoparticles

Analysis of the SEM images reveals that the synthesized nanoparticles exhibit both spherical and anisotropic (non-spherical) shapes. The particle size varies from 30 nm to 1 μm. Some particles have a width of approximately 700 nm and a length of ~1 μm. Additionally, smaller nanoparticles with sizes ranging from 20 to 100 nm are also observed.

Figure 2 displays surface images of irradiated and non-irradiated areas of MPG-6 carbon, obtained using scanning microscopy before and after laser exposure.

Comparison of the images shows that the surface nanolayer is significantly modified. The porous structure of the surface in the crater zone is clearly visible. This fine-crystalline material is a spatial network of crystallites, possibly with an amorphous intercrystallite boundary. It is likely that the surface destruction occurs more intensively from the intercrystallite phase. The observed changes in the relief of the surface layer of the sample subjected to laser action may be associated with a change in the phase composition. The results of studies of the modified surface by Raman scattering showed a change in the phase composition.

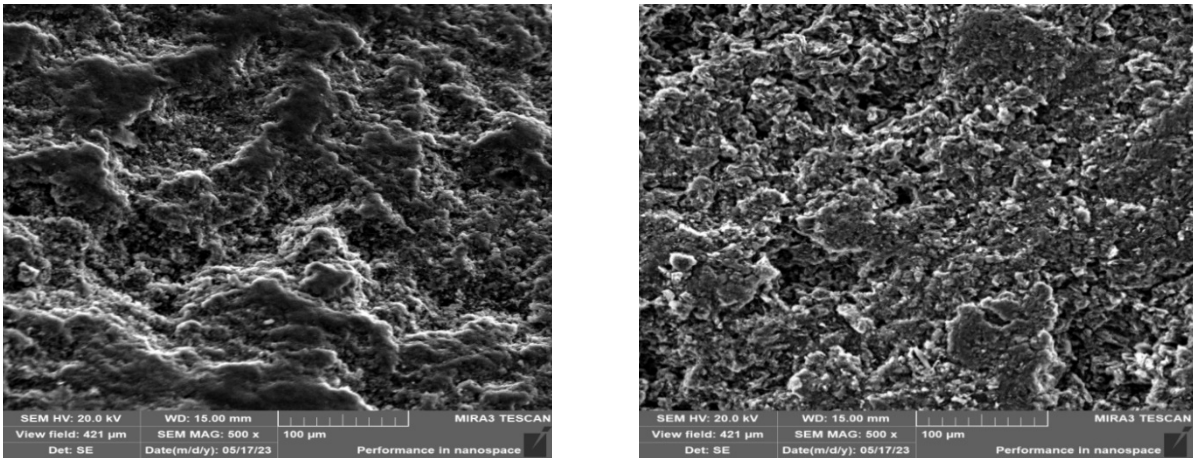

a - before irradiation *b* - after irradiation

Figure 2. Morphology of the surface of MPG-6 graphite before and after laser modification

We have carried out studies by the method of Raman scattering, the Raman spectra of graphite and the results of the decomposition of their spectral contour are presented (the Lorentz contour was used).

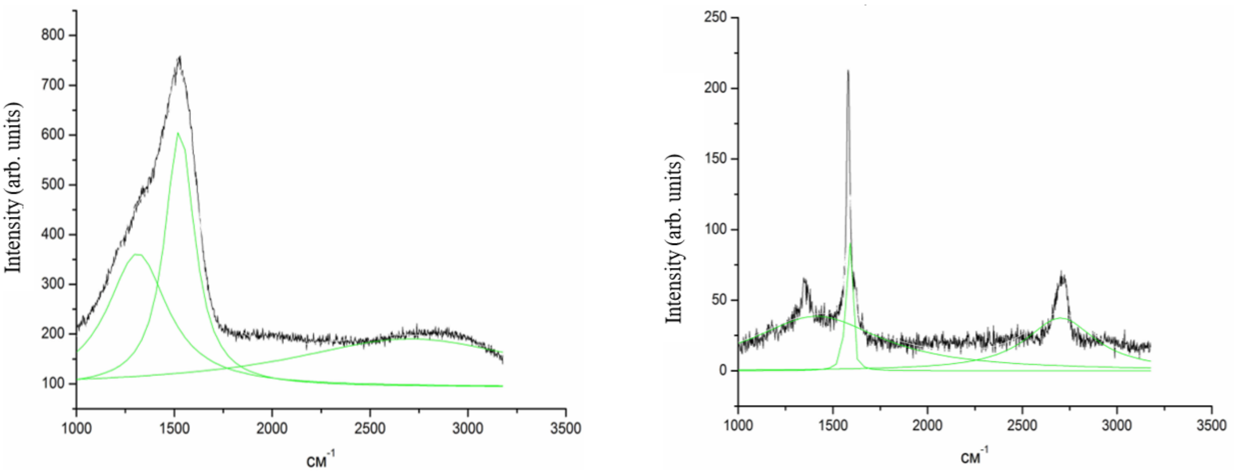

a) before laser treatment *b)* after laser treatment

Figure 3. Raman scattering spectra of MPG-6 graphite

The spectra before and after laser exposure differ significantly from each other. After exposure, three intense scattering bands are clearly visible in the spectrum. The appearance of a well-defined D line (~1354 cm^{-1}) is associated with inelastic scattering of excited electrons on phonons and elastic scattering of electrons on defects. The appearance of the D line indicates the presence of structural disorder in the ideal hexagonal structure (grain boundaries, defects, etc.). The 2D line (~2700 cm^{-1}) is not associated with the presence of structural defects and is present in most carbon materials with a graphite-like structure.

CONCLUSION

This study demonstrates the possibility of controlling the ablation process and the yield of carbon nanoparticles from an MPG-6 target in an aqueous medium. Effective generation of nanoparticles for use in various applications has been achieved. The morphology of nanoparticle conglomerates ranging in size from 30 nm to 1 μm has been studied. The shape of the particles is diverse. The surface of the MPG-6 crater is smooth, and the surface relief is significantly altered. The results of studies of the modified surface by Raman scattering showed a change in the phase composition.

ORCID

Amangeldi B. Kamalov, https://orcid.org/0000-0003-1460-0747; **Dauran J. Asanov,** https://orcid.org/0000-0003-0091-8105
Daryabay M. Esbergenov, https://orcid.org/0000-0002-7544-4031

REFERENCES

[1] C. Thamaraiselvan, J. Wang, D.K. James, P. Narkhede, S.P. Singh, D. Jassby, J.M. Tour, and C.J. Arnusch, "Laser-induced graphene and carbon nanotubes as conductive carbon-based materials in environmental technology," Materials Today, **34**, 115-131 (2020). https://doi.org/10.1016/j.mattod.2019.08.014

[2] R. Ye, X. Han, D.V. Kosynkin, Y. Li, C. Zhang, B. Jiang, A.A. Martí, and J.M. Tour, "Laser-induced conversion of teflon into fluorinated nanodiamonds or fluorinated graphene," ACS nano, **12**(2), 1083-1088 (2018). https://doi.org/10.1021/acsnano.7b05877
[3] S. Juodkazis, H. Misawa, T. Hashimoto, E.G. Gamaly, and B. Luther-Davies, "Laser-induced microexplosion confined in a bulk of silica: formation of nanocavities," Applied Physics Letters, **88**(20), 201909 (2006). http://dx.doi.org/10.1063/1.2204847
[4] F. Migliorini, S. Belmuso, D. Ciniglia, R. Dondè, and S. De Iuliis, "A double pulse LII experiment on carbon nanoparticles: insight into optical properties," Physical Chemistry Chemical Physics, **24**(33), 19837-19843 (2022). https://doi.org/10.1039/D2CP02639B
[5] K. Habiba, V.I. Makarov, B.R. Weiner, and G. Morell, "Fabrication of Nanomaterials by Pulsed Laser Synthesis," Manufacturing Nanostructures, **10**, 263-92 (2014). http://dx.doi.org/10.13140/RG.2.2.16446.28483
[6] E. Rodriguez, and L. Fernandez, "Role of laser parameters in the formation of carbon nanoparticles under dual-pulse irradiation," Optics Express, **30**(18), 25400-25410 (2022). https://doi.org/10.1364/OE.30.025400
[7] A. Rybaltovsky, E. Epifanov, D. Khmelenin, A. Shubny, Y. Zavorotny, V. Yusupov, and N. Minaev, "Two Approaches to the Laser-Induced Formation of Au/Ag Bimetallic Nanoparticles in Supercritical Carbon Dioxide," Nanomaterials, **11**(6), 1553 (2021). https://doi.org/10.3390/nano11061553
[8] Y. Shao, A. Pan, H. Yang, W. Zhang, X. Zhang, and G. Wang, "Formation mechanism of graphene quantum dots assisted by nitrogen and its application in detection of Hg^{2+}," Journal of Colloid and Interface Science, **512**, 777-785 (2018). https://doi.org/10.1016/j.jcis.2017.10.044
[9] F. Liu, and H.M Cheng, "Hydrothermal synthesis of graphene-based materials: Progress and challenges," Chemical Communications, **49**(50), 5203-5212 (2013). https://doi.org/10.1039/C3CC00165J
[10] O.O. Kurakevych, V.L. Solozhenko, and Y.L. Godec, "Single-crystal structures of carbon nitrides obtained by decomposition of melamine under high pressure," The Journal of Physical Chemistry C, **115**(45), 22392-22398 (2011). https://doi.org/10.1021/jp2073456
[11] J. Wang, X. Zhang, Y. Chen, and M. Sommerfeld, "Ultrafast formation of graphene on dielectric surfaces," Applied Physics Letters, **108**(11), 111602 (2016). https://doi.org/10.1063/1.4943961
[12] Z Wang, X. Lu, and C. Wang, "Laser-induced graphene: preparation, functionalization, and applications," Chemical Society Reviews, **44**(9), 2629-2642 (2015). https://doi.org/10.1039/C4CS00320G
[13] A. Kaczmarek, P. Denis, M. Krajewski, T. Mościcki, A. Małolepszy, and J. Hoffman, "Improved Laser Ablation Method for the Production of Luminescent Carbon Particles in Liquids," Materials, **14**(9), 2365 (2021). https://doi.org/10.3390%2Fma14092365
[14] O.A. Lazăr, A.S. Nikolov, C.C. Moise, and M. Enachescu, "Pulsed Laser Ablation in Liquids for Fabrication of Noble Metal Nanostructures," in: *Laser Ablation – Applications and Modeling*, edited by Dr. M. Harooni, (IntechOpen, 2023). http://dx.doi.org/10.5772/intechopen.111550
[15] D. Qi, X. Li, P. Wang, S. Chen, W. Huang, C. Li, K. Huang, et al., "Evolution of Laser-Induced Specific Nanostructures on SiGe Compounds via Laser Irradiation Intensity Tuning," **6**(1), 1-5 (2014). http://dx.doi.org/10.1109/JPHOT.2013.2294631
[16] A.G. Anisovich, A.P. Laskovnev, M.I. Markevich, A.N. Malyshko, and V.I. Zhuravleva, "Preparation of silicon and aluminum nanoparticles in an aqueous solution," Foundry production and metallurgy, (2), 76-80 (2021). https://doi.org/10.21122/1683-6065-2021-2-76-80. (in Russian)
[17] A.G. Anisovich, I.P. Akula, A.P. Laskovnev, M.I. Markevich, and N.M Chekan, "Creation and research of antistatic carbon coatings on fabric 05C8-KB, modified by metal clusters," Foundry production and metallurgy, (4), 113-117 (2020). https://doi.org/10.21122/1683-6065-2020-4-113-117. (in Russian)
[18] D.J. Asanov, "Pulse photon processing of a thin-film Si/Mg/Si/Sitall," System Science and Society scientific and methodological journal, (1), 4-6 (2023). (in Russian)
[19] M.I. Markevich, and D.J. Asanov, "Effect of laser radiation on photomagnetic materials based on silicon doped with impurities," in: *XV International Conference "Solid State Physics" (FTT-XV)*, (L.N. Gumilyov Eurasian National University, Astana, Kazakhstan, 2022), pp. 91-94.
[20] D.M. Esbergenov, E.M. Naurzalieva, and S.A. Tursinbaev, "Enhancing the perfection of a silicon crystal doped with nickel and zinc impurities," East European Journal of Physics, (4), 172-176 (2023). https://doi.org/10.26565/2312-4334-2023-4-19

ОСОБЛИВОСТІ ФОРМУВАННЯ ВУГЛЕЦЕВИХ НАНОЧАСТИНОК ПІД ВПЛИВОМ ЛАЗЕРА В РЕЖИМІ ГЕНЕРАЦІЇ ПОДВІЙНИХ ІМПУЛЬСІВ

Марія І. Маркевич[a], Амангельді Б. Камалов[b], Дауран Дж. Асанов[b], Дар'ябай М. Есбергенов[c], Манзура А. Казакбаєва[b]
[a]*Фізико-технічний інститут Національної академії наук Білорусі, Мінськ, Білорусь*
[b]*Нукуський державний педагогічний інститут імені Аджініяза, м. Нукус, Республіка Каракалпакстан*
[c]*Нукуський філіал Ташкентського університету інформаційних технологій імені аль-Хорезмі, Республіка Каракалпакстан*
У цьому дослідженні досліджується морфологія вуглецевих наночастинок, утворених шляхом абляції вуглецевої мішені MPG-6 у водному середовищі. У процесі абляції використовувався лазер на алюмінієво-ітрієвому гранаті LS-2134D (довжина хвилі: 1064 нм), що працює в режимі подвійного імпульсу (розділення імпульсів: 3 мкс, тривалість імпульсу: 10 нс, частота повторення імпульсу: 10 Гц, енергія одного імпульсу: ~ 0,05 Дж). Результати демонструють формування різноманітного діапазону вуглецевих наночастинок різного розміру та форми під час лазерної абляції. Крім того, дослідження демонструє здатність контролювати процес абляції та подальший синтез вуглецевих наночастинок, досягаючи ефективного генерування наночастинок, придатних для різних застосувань.
Ключові слова: *наночастинки; лазерне опромінення; наносекундна тривалість імпульсу; подвійний імпульсний режим; вуглець*